Supporting Information

Towards an Electronic Grade Nanoparticle-Assembled Silicon Thin Film by Ballistic Deposition at Room Temperature: Deposition Method, Structural and Electronic Properties.

*Giorgio Nava [a], Francesco Fumagalli [a], Salvatore Gambino [b], Isabella Farella [c], Giorgio Dell'Erba [a], Davide Beretta [a], Giorgio Divitini [d], Caterina Ducati [d], Mario Caironi [a], Adriano Cola [c], Fabio Di Fonzo [a,]***

[a] Center for Nano Science and Technology @PoliMI Istituto Italiano di Tecnologia, Via Giovannni Pascoli 70/3 Milano, 20133, (Italy).

[b] Dipartimento di Matematica e Fisica "Ennio De Giorgi", Università del Salento, Lecce, 73100, (Italy).

[c] Institute for Microelectronics and Microsystems—Unit of Lecce, National Council of Research (IMM/CNR), Via Monteroni 3/A, 73100 Lecce (Italy).

[d] Department of Materials Science and Metallurgy, University of Cambridge, 27 Charles Babbage Road, CB3 0FS Cambridge , (United Kingdom).

* Corresponding author: e-mail: fabio.difonzo@iit.it.

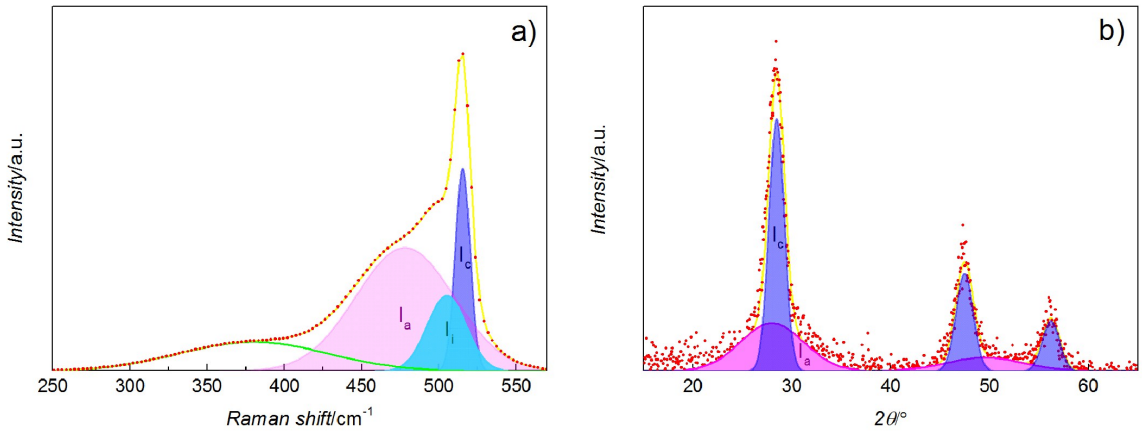

Figure S1. (a) Example of multi-peak fitting of Raman signal (crystalline, intermediate and amorphous TO components indicated by I_c, I_i and I_a respectively) and (b) of XRD signal (crystalline and amorphous components indicated by I_c and I_a) from NP-assembled silicon thin films

In order to extract information about the sample nanostructure a fitting routine was applied to the Raman signal in the region between 250 and 575 cm^{-1} according to the following procedure. Two peaks are employed for the Transverse Optical modes (TO modes) of the crystalline and amorphous phase, centered around 510-520 cm^{-1} and 480 cm^{-1} respectively, while the third peak is centered around 500-510 cm^{-1} and usually attributed to an intermediate crystalline component, assigned to strained silicon bonds on the nanocrystals surface or grain boundaries. [1-3] The aforementioned third Gaussian component can be better interpreted as a stratagem to account for the asymmetric broadening and displacement towards lower Raman shift values of the crystalline TO component upon nanoscale size confinement. [4, 5]

The grain size and crystalline fraction are derived from **Equation 1** and **Equation 2** respectively.

$$grain\ size[nm]:\ gs = 2\pi\sqrt{\frac{B}{\Delta\omega}} \qquad (1)$$

$$Crystalline\ volume\ fraction[\%]:\ cf = \frac{I_c + I_i}{I_c + I_i + \sigma I_a} \qquad (2)$$

Where I_c, I_a and I_i are the areas subtended by the crystalline, amorphous and intermediate components peaks (see **Figure S1a**), $\Delta\omega$ is the shift of the main crystalline component position with respect to the bulk crystalline silicon value, B = 2.0 cm^{-1} nm, σ is the ratio of the Raman cross section of amorphous and crystalline silicon (close to unity in the investigated range of grain sizes). [6]

A second Gaussian fit procedure was applied to the measured XRD spectra in the region between 15 and 65°. Three peaks are employed for the crystalline phase, corresponding to {111}, {220} and {311} lattice planes, and two for the amorphous one. The total area subtended by the crystalline and amorphous peaks are indicated by I_c and I_a (see Figure S11b). From the width of the {111} peak the average crystalline grain size was calculated from Scherrer's formula, reported in **Equation 3**.

$$gran\ size[nm]:\ gs = \frac{k\lambda}{\beta cos\theta} \qquad (3)$$

Where k=0.9, λ represent the wavelength of the impinging x-ray, β is the full width at half maximum of the {111} peak and θ is the angle at the center of the peak.

The crystalline volume fraction is derived from **Equation 4**.

$$Crystalline\ volume\ fraction[\%]: cf = \frac{I_c}{I_c + I_a} \quad (4)$$

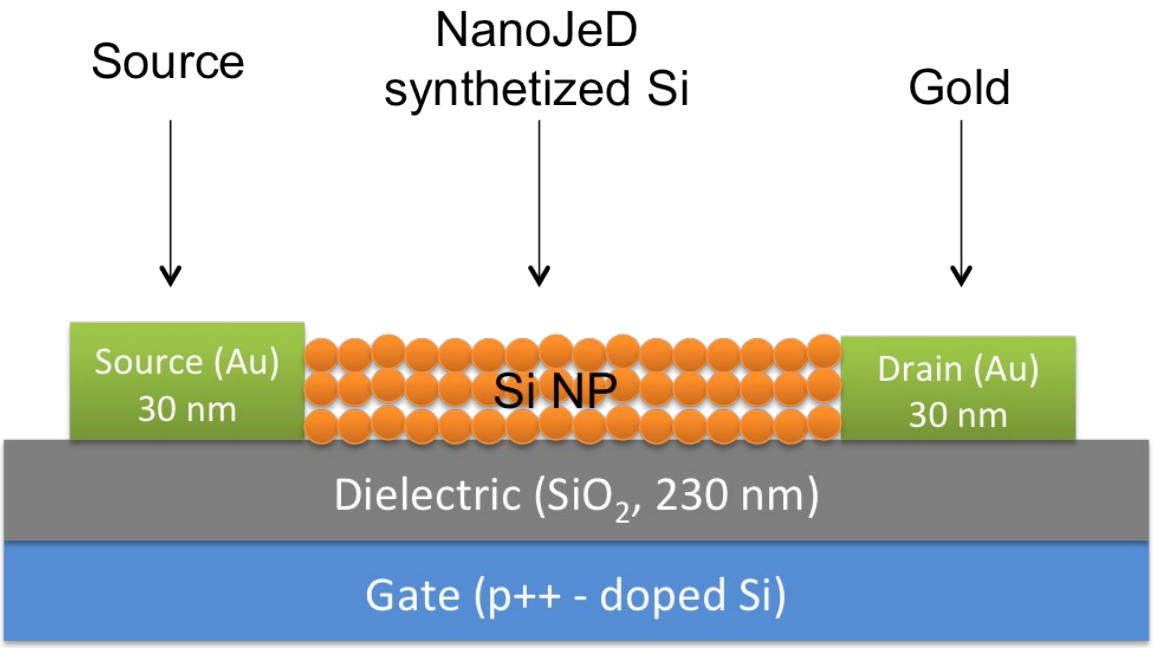

Figure S2. Schematics of the bottom-gate bottom-contacts configuration employed for the fabrication of the thin-film transistors. The pre-patterned silicon chips (Fraunhofer IPMS) structure consisted in a p-doped silicon gate (Si p+), 230 nm thick SiO_2 gate dielectric and 30 nm thick Au source and drain contacts. SNP-assembled thin films are directly synthetized via NanoJeD technique on top of the described structure.

For material analysis we used provides standardized single transistor structures in bottom gate architecture provided by Fraunhofer IPMS. These substrates for thin films field effect transistors (FETs) are prepared, with clean room quality, on silicon wafers with thermal silicon dioxide (SiO_2) as full-area dielectrics and gold electrodes in lift-off technology. In the standard pre-patterned layout layout, each 150 mm wafer has 960 individual transistors on 60 chips, each sized at 15 × 15 mm². Each chip carries four groups with four identical transistors, with a channel length of 2.5, 5, 10 and 20 µm respectively. More information about the specifics of the pre-patterned substrates can be found at the producer website (http://www.ipms.fraunhofer.de/content/dam/ipms/en/documents/end-of-line-substrates_web.pdf).

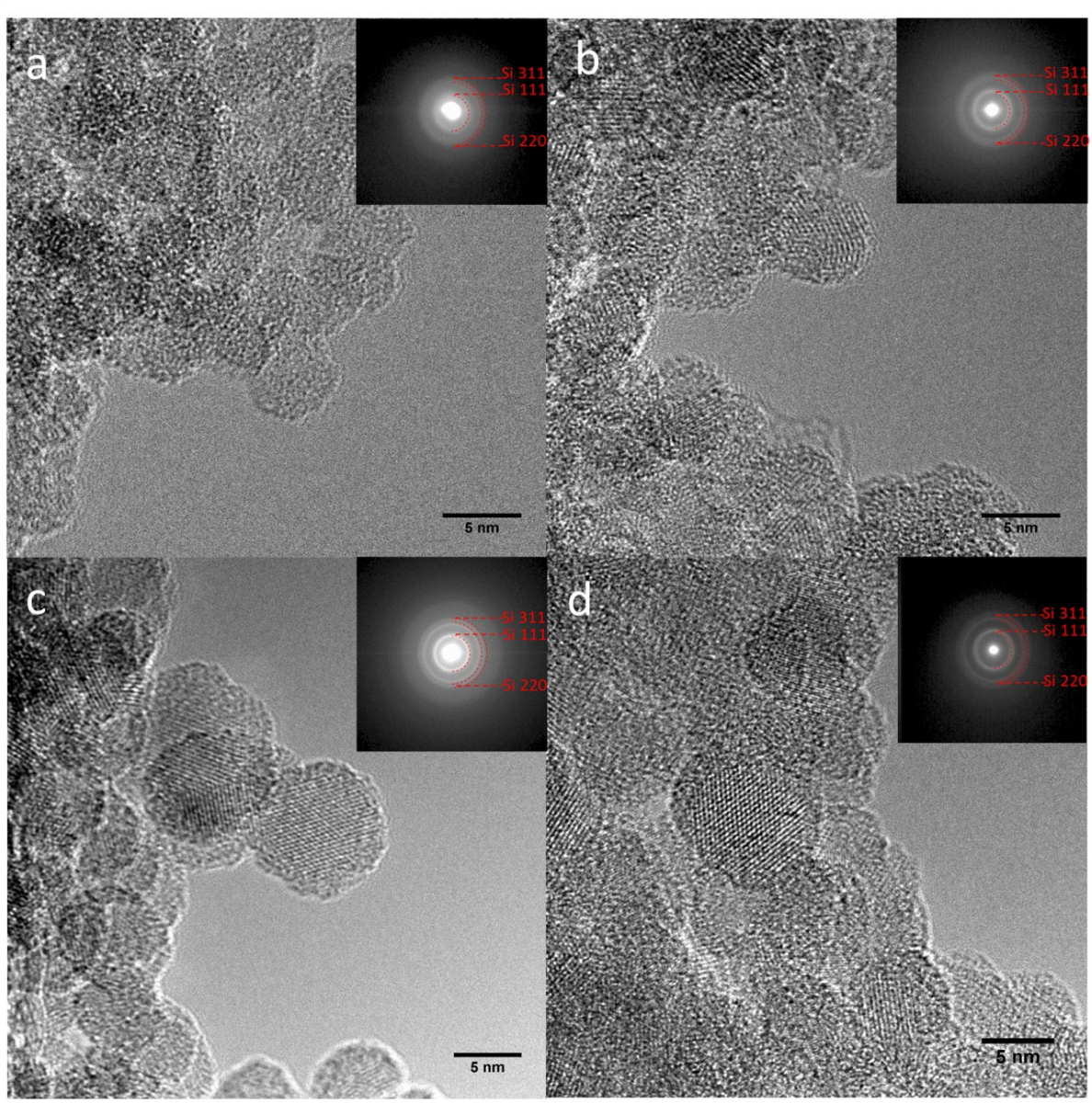

Figure S3. Bright field TEM micrographs of silicon-based nano-materials produced for different levels of RF power coupled into the plasma discharge: (a) 80 W, (b) 90 W, (c) 120 W and (d) 160 W. In the inset of panels b, c and d the progressive appearance of well-defined polycrystalline diffraction fringes can be distinguished.

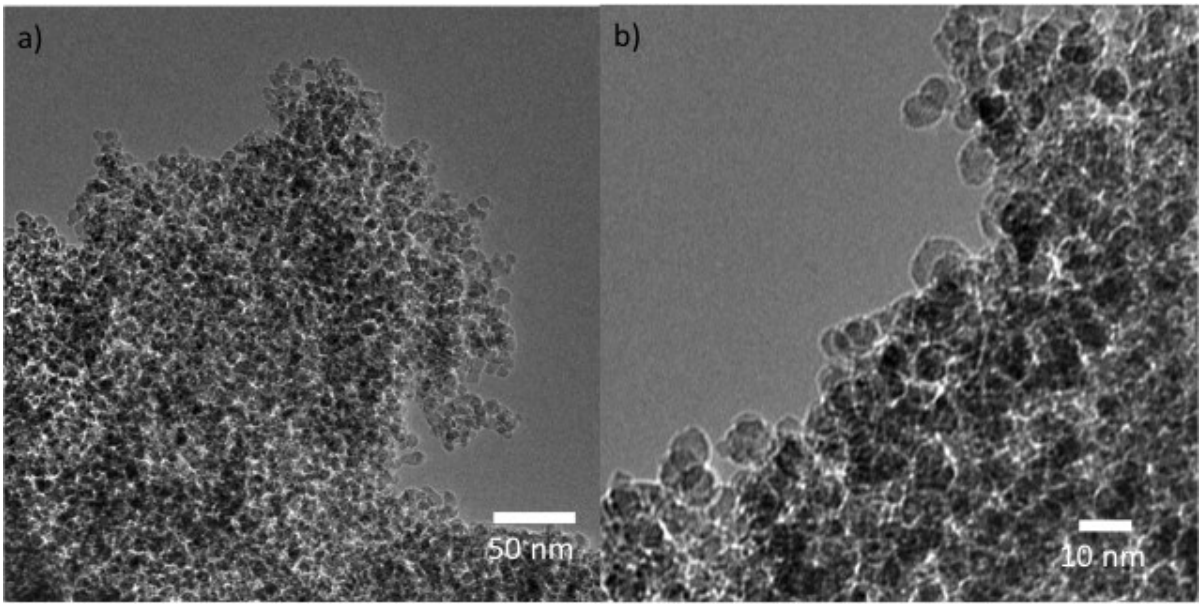

Figure S4. Low magnification bright field TEM micrographs of silicon-based nano-materials (delivered RF power was 120 W).

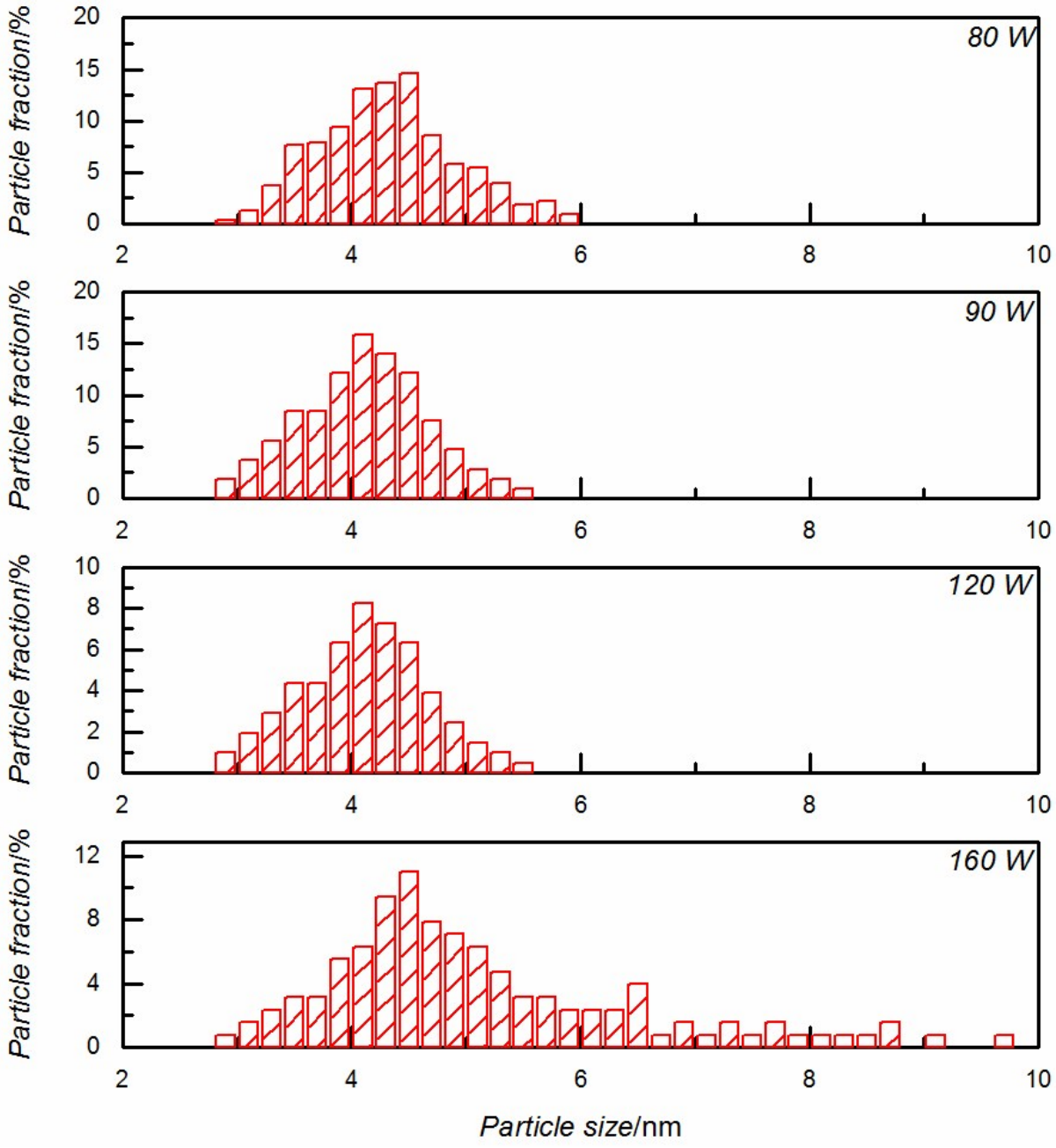

Figure S5. Nanoparticles size frequency count histograms as derived by statistical analysis of TEM micrographs. For each deposition condition particle diameters were derived directly from TEM micrographs via ImageJ analysis tools. Statistical ensembles analyzed were: 329 particles for SNP-assembled material deposited at 80 W, 107 particles for SNP-assembled material deposited at 90 W, 206 particles for SNP-assembled material deposited at 120 W and 127 particles for SNP-assembled material deposited at 160 W.

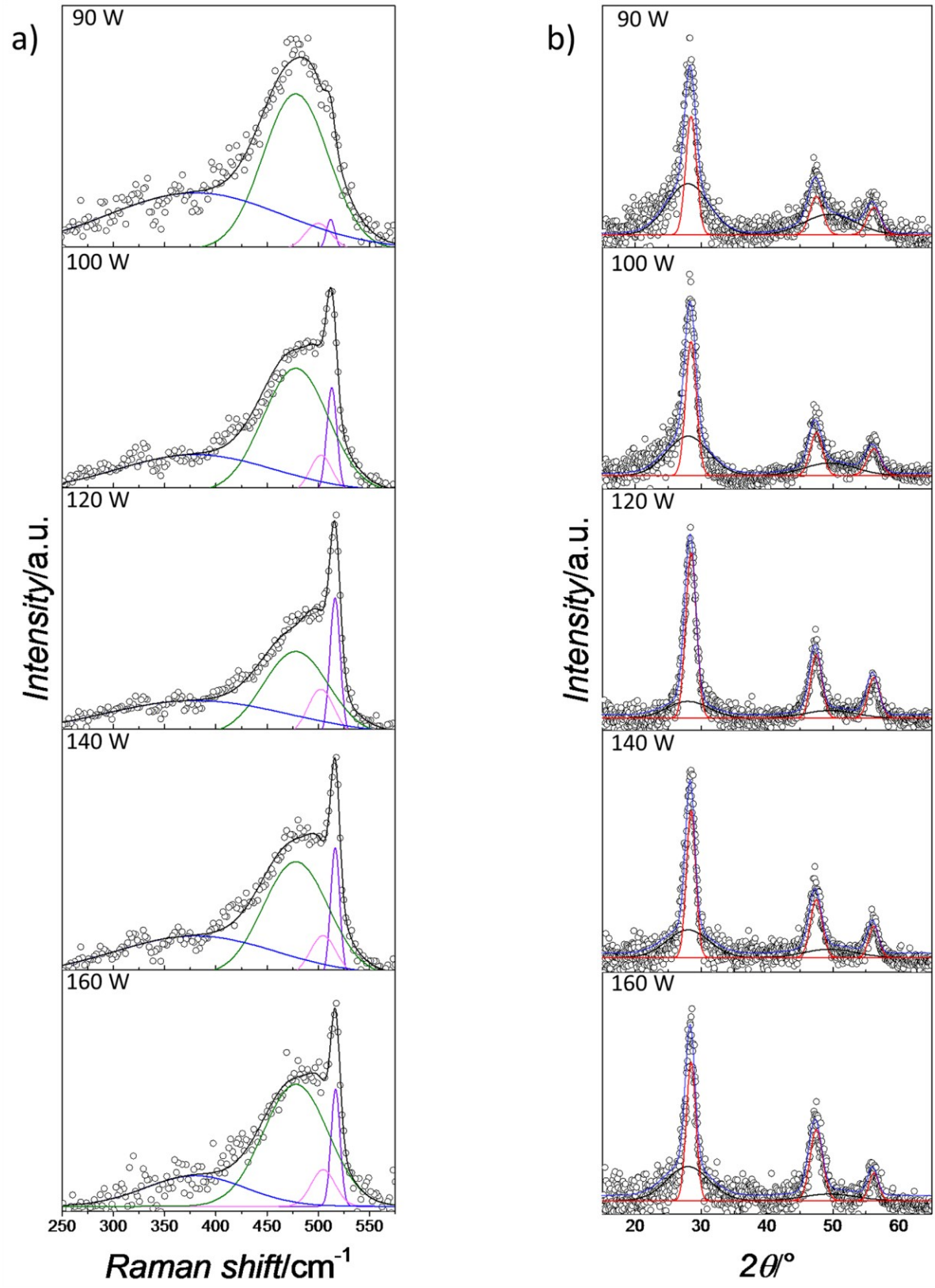

Figure S6. Raman spectra (a) of silicon nano-materials synthetized for increasing values of coupled RF power in the plasma discharge (black circles). The Gaussian peaks employed in the fitting routine (blue, green, pink and purple lines) and the resulting envelope curve (black line) are added as reference. Corresponding XRD spectra (b) of the synthetized silicon nano-materials (black circles). Gaussian peaks employed in the fitting routine (red and black lines)

and the resulting envelope curve (blue line) are added as reference. The value of the coupled RF power level is indicated.

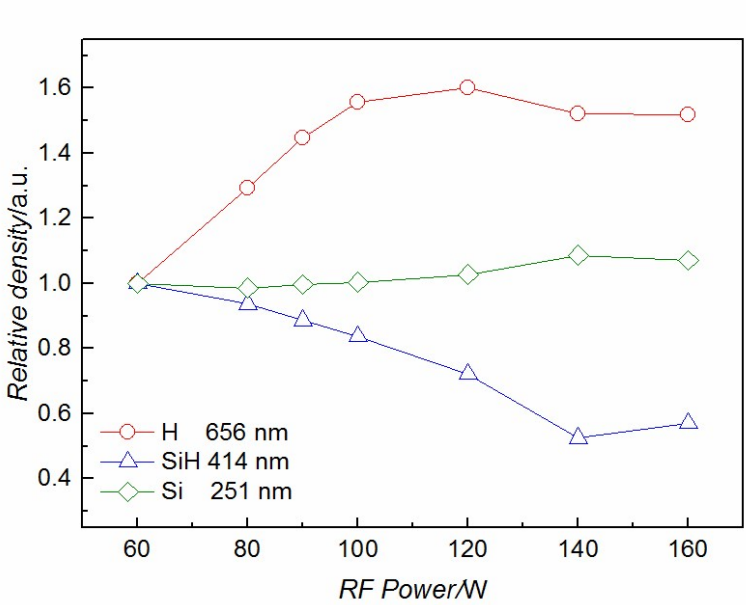

Figure S7. Relative ground state atomic and molecular densities of H, SiH and Si radicals as a function of RF power delivered in the discharge (estimated by optical emission spectroscopy using an actinometric technique).

Relative density variations of chemical species in the plasma were estimated by optical emission spectroscopy. Photon emission from the plasma discharge was characterized by means of Thorlabs CCS200 compact spectrometer equipped with a 3648- element linear CCD array, spectra range from 200 nm to 1000 nm and *FWHM* spectral accuracy < 2 nm at 633 nm. The optical emission was collected from the centre of the plasma environment along a line parallel to the electrode plates using an optical fiber mounted on a quartz viewport. All relative densities, being independent from each other, were normalized to the values recorded for 60 W RF power. Kr line at 826.3nm (E_{th} = 12.2 eV) emission intensity from the Paschen 2p2 level was used to normalize emission intensities of SiH at 414 nm, H at 656nm and Si at 251 nm. Actinometric measurements hypothesis were satisfied as a first approximation: the dominant mechanism for excitation of the Kr 2p2 level is a one-step electronic excitation from the ground state and, in addition its energy threshold for this process is (~12 eV), near the respective excitations of Si (~11 eV), H (~12 eV) and SiH (~10 eV). The actinometer used was introduced via dedicated line from a Kr bottle and its flow was kept under 5% of the total gas flow for all the experiments. Adding to the selected working gas mixture a small amount of Krypton in the range from 2% to 5% has been proven not to influence emission lines intensities of principal mixture components.

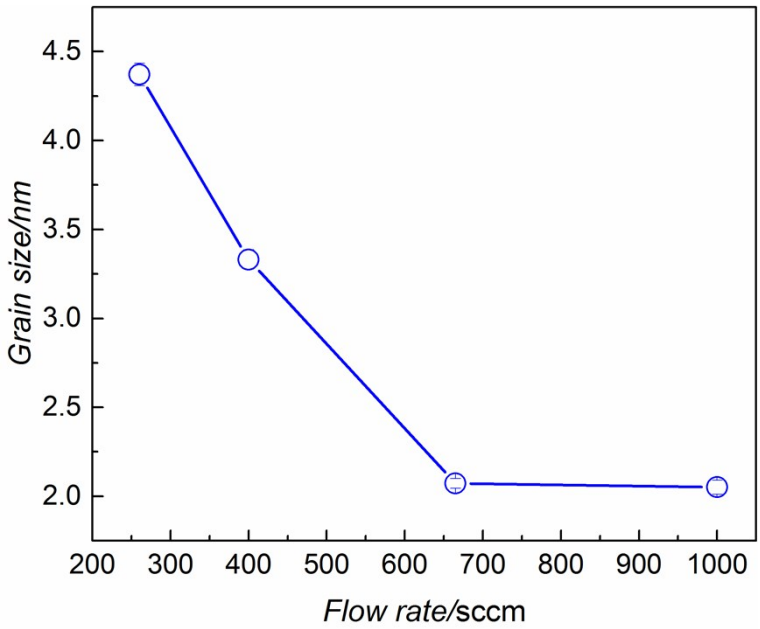

Figure S8. Crystalline grain size, as measured by XRD, of SNP-assembled films as a function of total gas flow rate ($[SiH_4]/[Ar+SiH_4]$=0.5%). NP's residence time in the plasma discharge decreases for increasing flow rate.

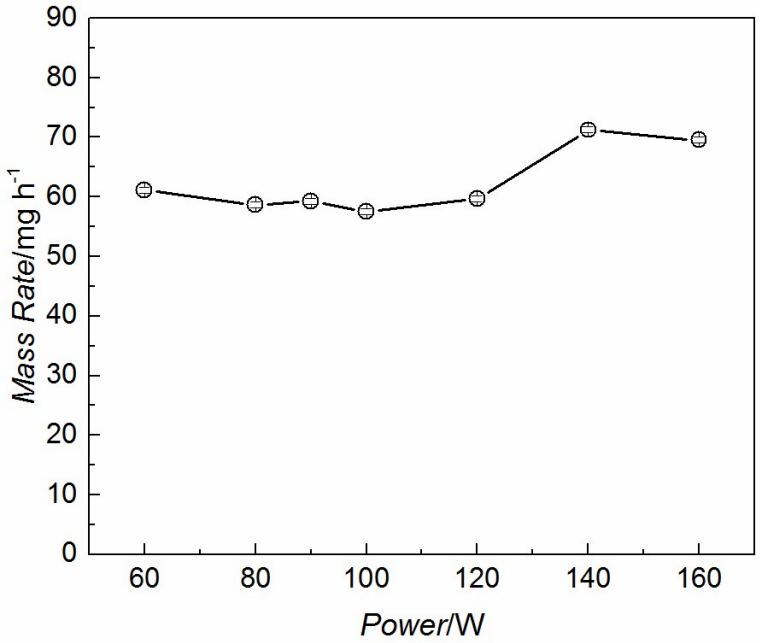

Figure S9. Variation of the absolute mass production rate of NP-assembled silicon thin films as a function of RF power input.

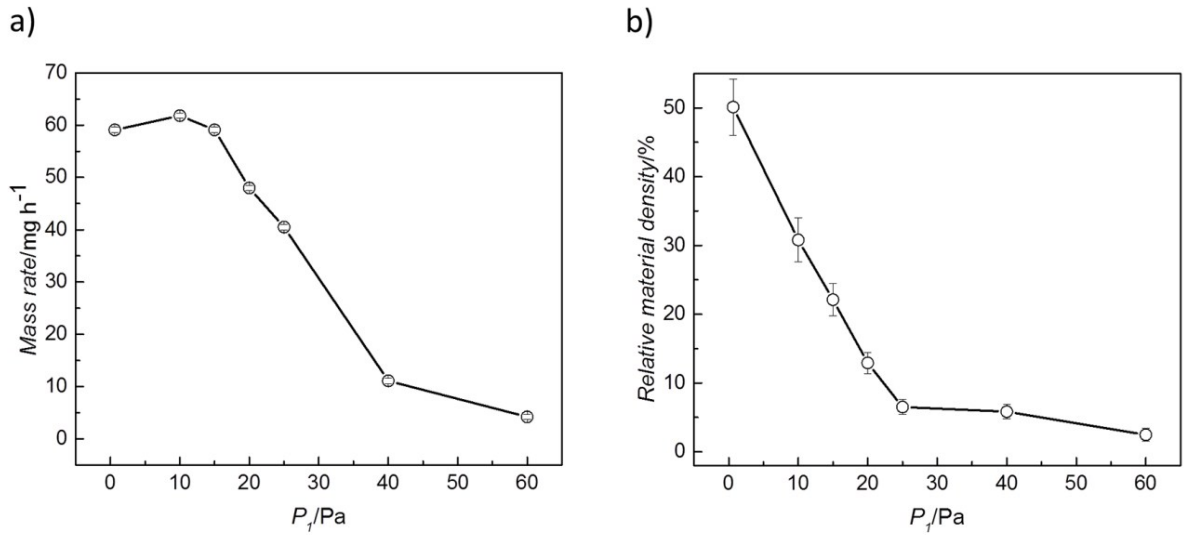

Figure S10. Variation of the absolute material mass deposition rate (a) and relative density (b) as a function of the total pressure of the impaction chamber.

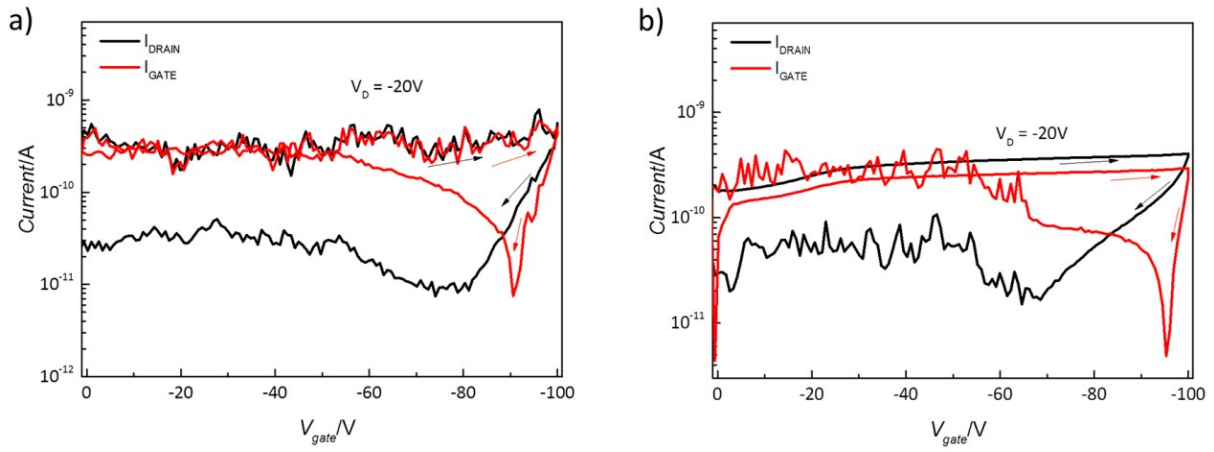

Figure S11. Plot of the transfer curve of SNP-assembled 10 µm (a) and 20 µm (b) long channel TFT devices: drain current (black) and gate leakage current curve (red). A drain voltage of -20 V was applied during the measurements. Arrows indicate the direction of the voltage sweep.

References:

[1] T. Lopez, L. Mangolini, *Nanoscale* **2014**, *6*, 1286.
[2] W. Li, D. Xia, H. Wang, X. Zhao, *J. Non-Cryst. Solids* **2010**, *356*, 2552.
[3] J. Gope, S. Kumar, A. Parashar, P. N. Dixit, C. M. S. Rauthan, O. S. Panwar, D. N. Patel, S. C. Agarwal, *J. Non-Cryst. Solids* **2009**, *355*, 2228.
[4] G. Faraci, S. Gibilisco, A. R. Pennisi, C. Faraci, *J. Appl. Phys.* **2011**, *109*, 074311.
[5] G. Faraci, S. Gibilisco, P. Russo, A. R. Pennisi, S. La Rosa, *Phys. Rev. B* **2006**, *73*, 033307.
[6] T. Cao, H. Zhang, B. Yan, Y. Cheng, *RSC Adv.* **2013**, *3*, 20157.